Bazyli KRUPICZ[*]**, Piotr ZASTOCKI**[**]**, Paweł KRUPICZ**[***]

EROSION OF TUBULAR HEAT EXCHANGERS

EROZJA KAWITACYJNA RUROWYCH WYMIENNIKÓW CIEPŁA

Key words:	cavitation, steam condenser, top head of the condenser, flow simulation.
Abstract:	This paper presents the results of an erosion study of a tubular heat exchanger operating on a railroad sleeper saturation processing line. The object of the study is a DN 800 oil condenser cooling the creosote oil vapors flowing through the condenser tubes, fixed in the sieve plates located in top head and bottom head of the condenser. Subject to the erosion are the upper part of the tubes and the weld connecting the tubes to the upper sieve plate. This resulted in unsealing of the connection, which led to the contamination of the cooling medium. The key problem, therefore, is to protect the entire top head of the condenser from erosion. Since only the central part of the surface of the top sieve plate was eroded, the conclusion is that the velocity of the vapor stream over the inlet to the condenser tubes in the central part and beyond is varied. This thesis was confirmed by the correspondence of the actual eroded area with the cavitation area resulting from a simulated flow in Autodesk CFD 2019 Ultimate software after increasing the height of top head of the condenser, placing a stream dispersing element between the liquid vapor inlet to the condenser and the upper sieve plate, and after applying a protective sieve plate. Flow simulation studies for each of these variants, or a combination of them, made it possible to evaluate the tested solutions in terms of protection against erosion, including cavitation erosion, of the upper sieve plate of the condenser.
Słowa kluczowe:	kawitacja, kondensator pary, dennica kondensatora, symulacja przepływów.
Streszczenie:	W pracy przeprowadzono analizę erozji kawitacyjnej rurowego wymiennika ciepła pracującego na linii technologicznej nasycania drewna. Obiektem badań jest kondensator oleju DN 800 schładzający pary oleju kreozotowego przepływające przez rurki kondensatora zamocowane w płycie sitowej dennicy górnej i dolnej. Intensywną erozją kawitacyjną była objęta powierzchnia górnej płyty sitowej znajdującej się bezpośrednio nad wlotem par cieczy do kondensatora. Erozji ulega górna część rurek oraz spaw łączący rurki z górną płytą sitową. W efekcie powstawało rozszczelnienie połączenia, którego następstwem było skażenia czynnika schładzającego. Kluczowym problemem jest więc ochrona przed kawitacją całej dennicy kondensatora. Ponieważ erozji podlegała tylko część centralna powierzchni górnej płyty sitowej, stąd wniosek, że prędkość strumienia pary nad wlotem do rurek kondensatora w części centralnej i poza nią jest zróżnicowana. Potwierdzeniem tej tezy była zgodność rzeczywistego obszaru objętego erozją z miejscem kawitacji wynikającym z symulacyjnego przepływu w programie Autodesk CFD 2019 Ultimate. W tym programie zbadano również, jak zmienia się ciśnienie i prędkość przepływu par cieczy w dennicy górnej po modernizacji dennicy górnej w kilku wariantach, polegających na: podwyższeniu wysokości dennicy górnej, umieszczeniu elementu rozpraszającego strugę między wlotem par cieczy do kondensatora i górną płytą sitową, zastosowanie ochronnej płyty sitowej. Badania symulacyjne przepływu dla każdego z tych wariantów lub ich połączenie pozwalają ocenić badane rozwiązania pod kątem ochrony przed erozją kawitacyjną górnej płyty sitowej kondensatora.

INTRODUCTION

Cavitation occurs locally during the flow of a liquid in an area, where its vapor pressure is reached. This may occur when the velocity of the liquid flow passing an obstacle suddenly increases and a rapid pressure drop is induced in this area **[L. 1, 2, 3, 4].** Cavitation also occurs on rotor blades of pumps operating at high rotational speed. Its cause is a significant difference in the velocity of the liquid at the end of the blade and in its surroundings, and thus also a large difference in

---

[*] ORCID: 0000-0001-7703-9913. Bialystok University of Technology, Faculty of Engineering Management, Wiejska 45A, 15-351 Białystok, e-mail: b.krupicz@pb.edu.pl.

[**] Bialystok University of Technology Graduate, Faculty of Engineering Management, Wiejska 45A, 15-351 Białystok.

[***] ORCID: 0000-0002-7028-8244. Stangl Technik Polska Sp. z o.o., Poland.

pressure [L. 5, 6, 7]. A similar phenomenon occurs in the bends of pipelines, where the liquid is subject to a rapid change in the direction of the flow and a local change in velocity and pressure. Erosion is often accompanied by chemical corrosion. Noise, on the other hand, is a characteristic of cavitation erosion [L. 8, 9, 10]. Conditions for the occurrence of cavitation can also be met in tubular heat exchangers, when there is a large temperature difference on both sides of the tubes, through which the heat exchange takes place. Then, at the partition on the side of the liquid receiving heat, an evaporation may occur locally and the resulting vapor bubbles will implode among the flowing liquid or upon collision with an obstacle [L. 11]. The DN800 type liquid vapor condenser is also a tubular heat exchanger, in which erosion occurs at the liquid vapor inlet to the condenser tubes. The purpose of this study is to identify the erosion of a DN800 liquid vapor condenser used in a railroad sleeper saturation processing line, and to evaluate the impact of how the sieve plate and condenser tubes can be protected from erosion using flow simulation in Autodesk CFD 2019 software.

IDENTIFICATION OF THE PROBLEM

Erosion wear of the DN800 type liquid vapor condenser, as a component of a processing line for saturating railway sleepers with creosote oil, is one of the main operational problems of this line [L. 12]. Fig. 1 shows a simplified diagram of a processing line for saturating wood with creosote oil.
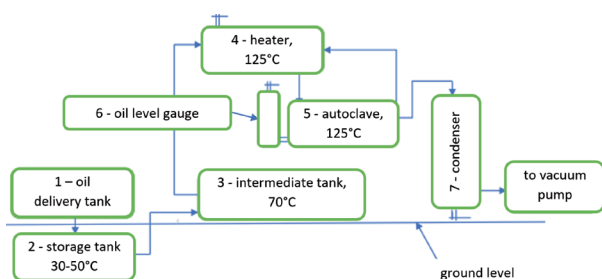

Fig. 1. Flow diagram of creosote oil in a railway sleeper saturation processing line: 1 – delivery tank, 2 – storage tank, 3 – intermediate tank, 4 – heater, 5 – wood autoclave, 6 – oil level gauge, 7 – oil vapor condenser

Rys. 1. Schemat przepływu oleju kreozotowego w linii technologicznej nasycania podkładów kolejowych: 1 – cysterna dostawcza, 2 – cysterna magazynująca, 3 – zbiornik pośredni, 4 – podgrzewacz, 5 – autoklaw z drewnem, 6 – miernik poziomu oleju, 7 – kondensator par oleju

Creosote oil is a fraction of coal tar. The boiling point of oil is in the range of 200–360°C. For the impregnation of wood, oil with the trade name of Creosote EN 13991WEI-C is used, which crystallizes below a temperature of 30°C. Hence, the temperature of the oil in the delivery and storage tanks is maintained at 30°C–50°C. In the event of an oil spill outside the plant, where the temperature is <30°C, the oil is cooled and crystallizes, ensuring that no environmental contamination will occur. Fig. 2 shows a view of the stacked wood in the cylinder (autoclave). The saturation proceeds according to the Rüping method [L. 13]. It is a vacuum-pressure saturation, resulting in saturation of the wood throughout its volume. The pressure value and the saturation time are adapted to the type of wood and its moisture content. Depending on the current demand, the oil is taken from storage tank 2 (Fig. 1) to intermediate tank 3, where a temperature of 70°C is maintained. Prior to saturation, an overpressure of 0.2 MPa is generated in tanker 3. Under its influence the oil is pushed into tanker 4 and heated to 125°C. During heating, the tank outlet at its top is open, hence there is atmospheric pressure in the tank. The temperature of 125°C is reached after evaporation of water from the oil.

Fig. 2. View of the wood stacked in the autoclave [L. 14]
Rys. 2. Widok ułożonego drewna w autoklawie [L. 14]

Once the cylinder (autoclave) is loaded with wood (5), a partial vacuum of up to – 0.08 MPa is generated in the cylinder. The wood is dried in these conditions, then the cylinder is filled with 125°C oil dripping from heater 4 (Fig. 1). Using the communicating vessels principle, the oil level in the cylinder is observed in a tank connected in parallel (6). In the next stage, an overpressure of up to 0.8 MPa is generated and the actual saturation takes place. The saturation time depends
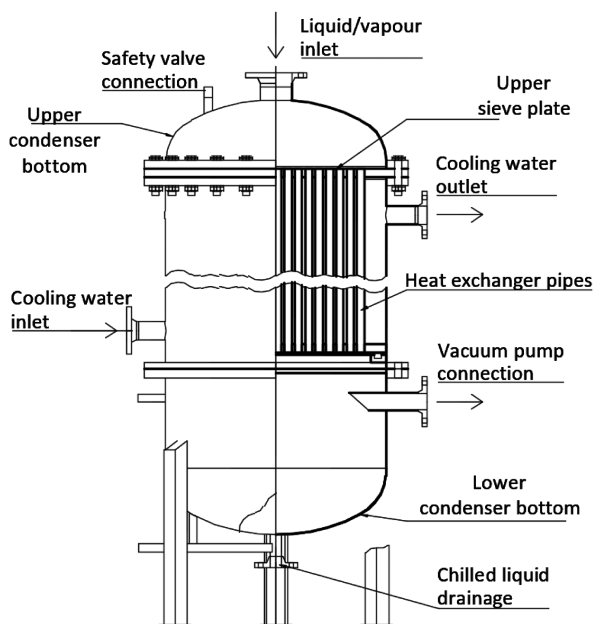
Fig. 3. Condenser diagram
Rys. 3. Schemat kondensatora

mainly on the moisture content of the wood. The elimination of the overpressure is linked to the removal of the oil from the autoclave. The residual oil-water mixture vapor from the wood is routed via a pipeline to condenser 7 (**Fig. 1**) under partial vacuum conditions down to -0.08 MPa. A diagram of the condenser construction is shown in **Fig. 3**.

The condensation of oil vapors takes place as they flow through the condenser tubes, located between the upper and lower sieve plates. The tubes are arranged in a 60° hexagonal pattern, shown in **Fig. 4a**. Traces of erosion (**Fig. 4b**) can be seen at the oil vapor inlet to the tubes in the central part of the upper sieve plate. Damage to the welds, resulting from the erosion of connections between the tubes and the top head of the condenser, was the cause of the connection being unsealed and cooling water entering the tubes, where the oil/water vapor mixture flow.

The questions are: why only the central part of the top head of the condenser is eroded, are the tubes inside also eroded and how to reduce or eliminate this phenomenon.
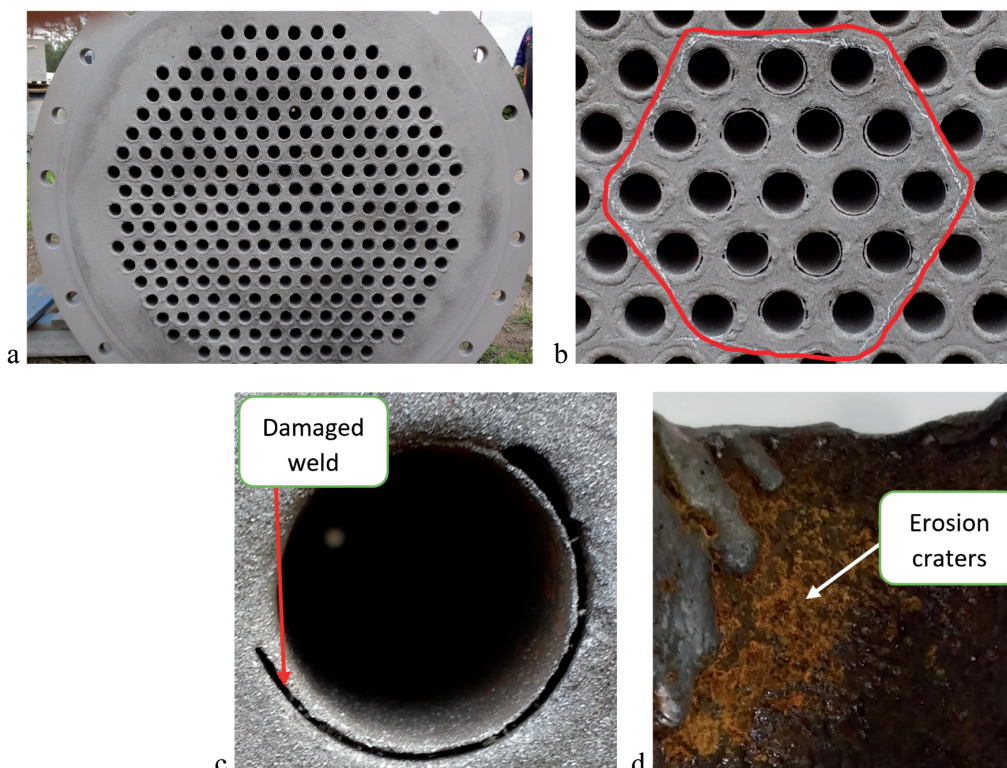

Fig. 4. a – arrangement of the tube inlet in the top head of the condenser, b – traces of erosion in the central part of the top head of the condenser, c – damaged connection between the tube and the top head of the condenser, d – traces of cavitation erosion in the tube on the side of the upper sieve plate
Rys. 4. a – rozmieszczenie wlotu rurek w dennicy górnej, b – ślady erozji kawitacyjnej w centralnej części dennicy, c – zniszczone połączenie rurki z dennicą górną, d – ślady erozji kawitacyjnej w rurce od strony górnej płyty sitowej

ANALYSIS OF CAVITATION WEAR
IN THE DN800 CONDENSER

The technical condition of the tubes was assessed after dismantling the condenser shell. The tubes on the external side showed no signs of erosion. To determine the damage on the inner side of the tubes, 10 samples were taken from the eroded area (**Fig. 4b**) on the vapor inlet side. The state of damage was assessed on the basis of the type of erosion traces and the results of tube wall thickness measurements at three cross-sections every 20 mm from the vapor inlet and at a fourth cross-section 20 mm from the vapor outlet. The locations of the tube wall thickness measurements are indicated in **Fig. 5**. Measurements were taken using electronic caliper. Traces of erosion craters with sharp edges in the tube (**Fig. 4d**) are characteristic of cavitational erosion. The top head of the condenser was also eroded, especially its central part. Intense erosion defects were formed at the vapor inlet to the condenser tubes, including the welded connection between the tubes and the top sieve plate (**Fig. 4c**). The type of surface formed, combined with the intensity of the erosion, indicates that this may be the result of the synergistic influence of the erosive particle stream of the flowing creosote oil/water vapor mixture and cavitational erosion.
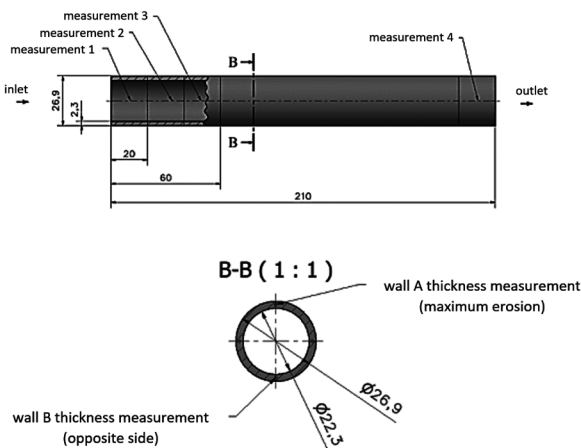

Fig. 5. **Diagram of the tube with the indicated location of the wall thickness measurement [L. 14]**
Rys. 5. Próbka rurki kondensatora ze wskazaniem miejsca pomiaru (A) grubości ścianki rurki **[L. 14]**

The wall thickness of the tubes at their circumference was found to be varied. The smallest wall thicknesses, corresponding to the maximum cavitational wear, were taken for analysis (**Fig. 5**, point A). The results of the wall thickness loss measurements in the test specimens are shown in **Fig. 6**.
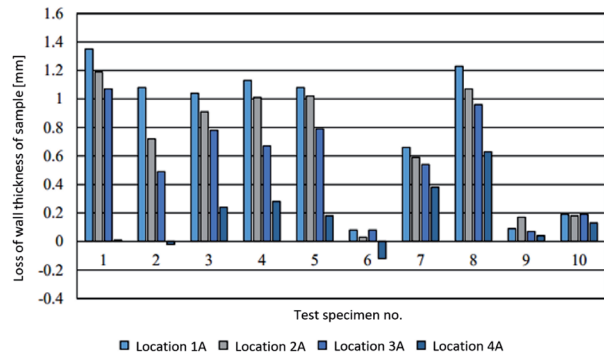

Fig. 6. **Tube wall thickness loss results, obtained from measurements in four sections (1A, 2A, 3A, 4A) in 10 tubes [L. 15]**
Rys. 6. Wyniki utraty grubości ścianki rurki, uzyskane z pomiarów w czterech przekrojach (1A, 2A, 3A, 4A) w10 rurkach **[L. 15]**

Data shown in **Fig. 6** indicate, that cavitational erosion affects not only the welds connecting the tubes to the top head of the condenser at the central part of the tube, but it also occurs in the tubes at a length of about 60 mm. The values of measurements 4A, regarding the area close to the oil outlet of the tube, practically do not exceed 0.2 mm in all samples and have reached negative values in two samples. These may be due to dimensional imperfections in the tubes, corrosion or local permanent contamination. The occurrence of cavitation in this area of the tubes is hampered by the fact that oil in vapor form is practically no longer present there and the flow conditions are fixed.

Under the partial vacuum conditions of -0.08 MPa in the cylinder and a temperature of 235°C, a mixture of oil and steam washed from the wood flows into the condenser. The vapor bubbles, colliding with the edges of the tubes and the surrounding weld, lose velocity, but at the same time the pressure in their surroundings increases, which causes the bubbles to implode. Further on, the vapor particles fall into the tubes and, as a result of the continuity of the stream, their velocity increases and the pressure is thereby reduced. Conditions are thus created for the formation of new vapor bubbles, mainly water. The bubbles reduce their velocity by the tube walls and thus the pressure in their surroundings increases, which is the reason for the implosion of the bubbles **[L. 15, 16, 17, 18]**.

ANALYSIS OF THE RESULTS
OF NUMERICAL CALCULATIONS
OF WATER FLOW IN DN800 CONDENSER

The analysis of the fluid flow in the DN800 condenser was carried out by a computer simulation using Autodesk Inventor Professional 2018 and additional CFD 2019 Ultimate software for numerical calculations. The program makes it impossible to combine the simultaneous flow of several fluids with different physical properties. During the saturation process, water is pushed out of the wood. When the saturation is complete, the resulting oil-water mixture flows from the cylinder into the heater (5, **Fig. 2**). The residual mixture remaining in the cylinder and on the wood, in partial vacuum conditions, flows into the condenser. Due to the much lower evaporation temperature of water compared to the evaporation temperature of creosote oil, it is the water that causes cavitational erosion of the upper sieve plate. Hence, the numerical calculations focus on the water flow. The distribution of the average flow velocity and static pressure in the top head of the condenser was investigated with different modifications to the condenser design. The aim of this analysis is to look for ways to eliminate or mitigate the cavitational erosion **[L. 18, 19].** Based on the technical documentation, a model reflecting the actual appearance of the DN 800 oil condenser was developed in Autodesk Inventor Professional 2018 software. The finished model was transferred for analysis in CFD 2019 Ultimate. In this program the materials of the tubes, tank heads, shell, threaded connections, seals and stub pipes were assigned. The boundary conditions applied to the flowing medium at the inlet and outlet of the heat exchanger. An outlet partial vacuum of -7 kPa and a temperature of 90°C was used.

Figures 7–14 show the distribution of flow velocity and water pressure in the top head of the condenser, before and after design changes to reduce or eliminate cavitational erosion in the top head area of the condenser.
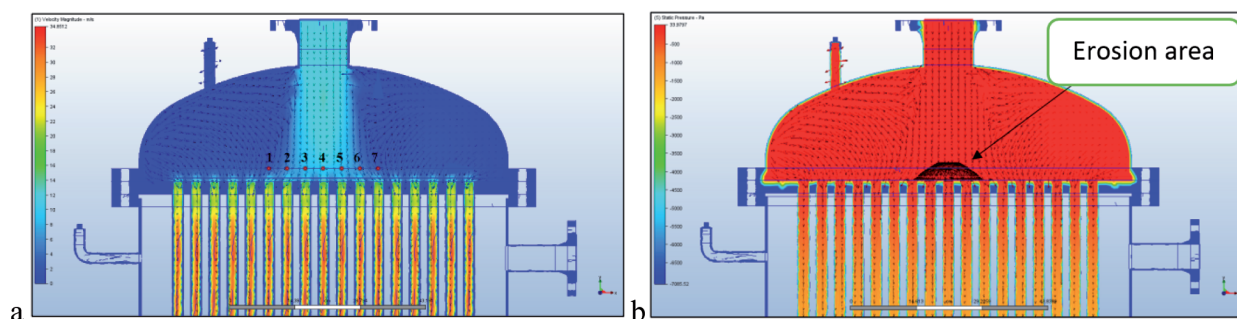

Fig. 7. **Distribution of water flow velocity (a) and pressure (b) in the top head area of the condenser without design changes**
Rys. 7. Rozkład prędkości przepływu wody (a) i ciśnienia (b) w dennicy górnej kondensatora bez zmian konstrukcyjnych

Based on the computational data of the flow simulations shown in **Figure 7**, one can assume that the distribution of velocity and thus pressure over the sieve plate varies. The highest velocity values are reached in the central part of the plate. These are sufficient to cause cavitation at the inlet to the condenser tubes. This confirms that cavitational erosion occurs at this location in the capacitor in service. Design changes in the area of condenser top head, which will result in uniform flow conditions over the condenser tubes, will result in lower velocities. If these values are lower than critical, cavitation will not occur. Following variants of dispersing the oil stream were tested: increased height of the top head of the condenser, use of an additional dispersion plate, use of a falling droplet shaped dispersion element and use of additional PA66 polyamide laying on sieve plate.

The flow simulation results for the distribution of water flow velocity and pressure in the top head area of the condenser after increasing its height by 150 mm and 250 mm are shown in **Fig. 8** and **Fig. 9**, respectively.

The distribution of water flow velocity and pressure in the top head area of the condenser after increasing its height by 50 mm was also studied. The distribution characteristics of these quantities were similar to those where the height
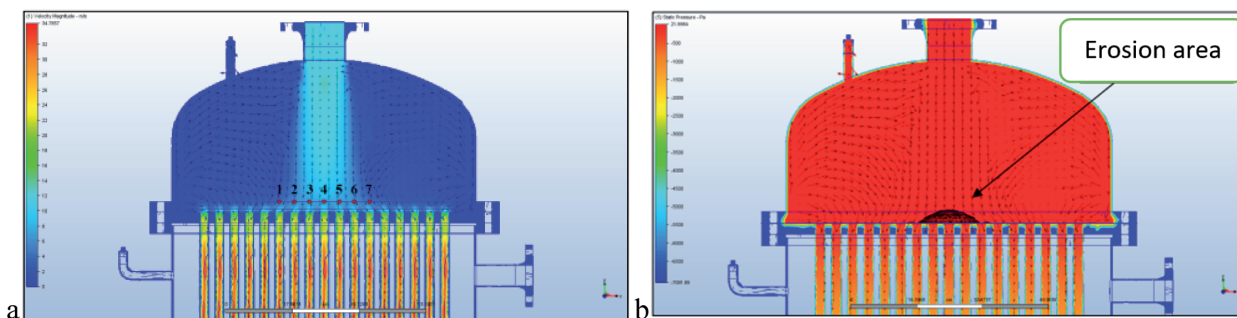
Fig. 8. Distribution of water flow velocity (a) and pressure (b) in the top head area of the condenser after increasing its height by 150 mm

Rys. 8. Rozkład prędkości przepływu wody (a) i ciśnienia (b) w dennicy górnej kondensatora po zwiększeniu jej wysokości o 150 mm
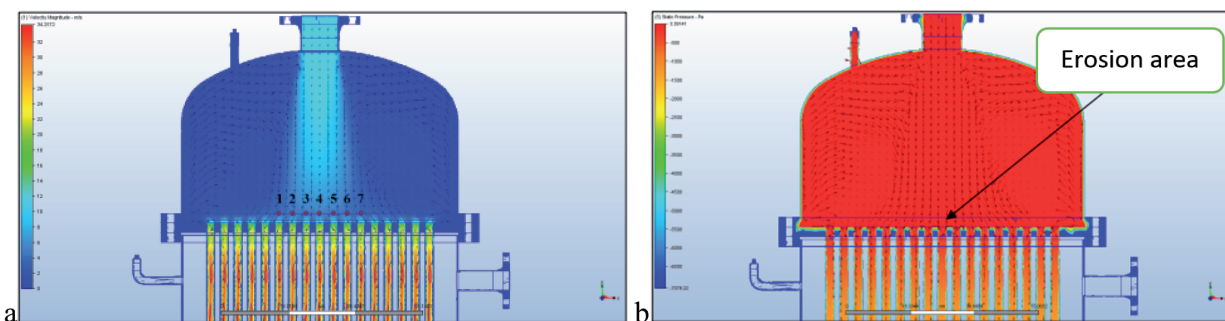

Fig. 9. Distribution of water flow velocity (a) and pressure (b) in top head area of the condenser after increasing its height by 250 mm

Rys. 9. Rozkład prędkości przepływu wody (a) i ciśnienia (b) w dennicy górnej kondensatora po zwiększeniu jej wysokości o 250 mm

was increased by 150 mm (**Fig. 8**). Increasing the height of the top head of the condenser by 250 mm does not guarantee a uniform distribution of velocity and pressure over the sieve plate (**Fig. 9**), but it does reduce the velocity below a value that does not cause cavitation.

Next tested variant was a steel dispersion plate placed halfway up the top head of the condenser. The effects of stream dispersion in the top head of the tank, with dispersion plate and no change in height, are shown in **Fig. 10** and, with dispersion plate and after increasing the height by 250 mm, in **Fig. 11**. In both cases the simulated flow shows no cavitation over the sieve plate, but the dispersion plate undergoes intensive cavitational erosion. Its service life will be limited.

The effects in next tested variant of the stream dispersion in top head of the condenser elevated by 250 mm with a falling droplet shaped element, in the stream flow simulation tests are shown in **Fig. 12**. The stream shows a uniform velocity and pressure distribution over the sieve plate compared to the

flow without the dispersion element (**Fig. 9**). The simulated stream flow does not show cavitation at the sieve plate, but cavitation can occur at the top of the dispersion element. The disadvantages of using dispersion elements are that they have to be fixed in the space between the stream inlet to the condenser and the sieve plate, and they have a limited lifetime due to cavitational erosion.

The effects of the stream dispersion in the upper condenser bottom elevated by 250 mm with a falling droplet shaped element, in the stream flow simulation tests are shown in **Fig. 12**. The stream shows a uniform velocity and pressure distribution over the sieve plate compared to the flow without the dispersion element (**Fig. 9**). The simulated stream flow does not show cavitation at the sieve plate, but cavitation can occur at the top of the dispersion element. The disadvantages of using dispersion elements are that they have to be fixed in the space between the stream inlet to the condenser and the sieve plate, and they have a limited lifetime due to cavitational erosion.
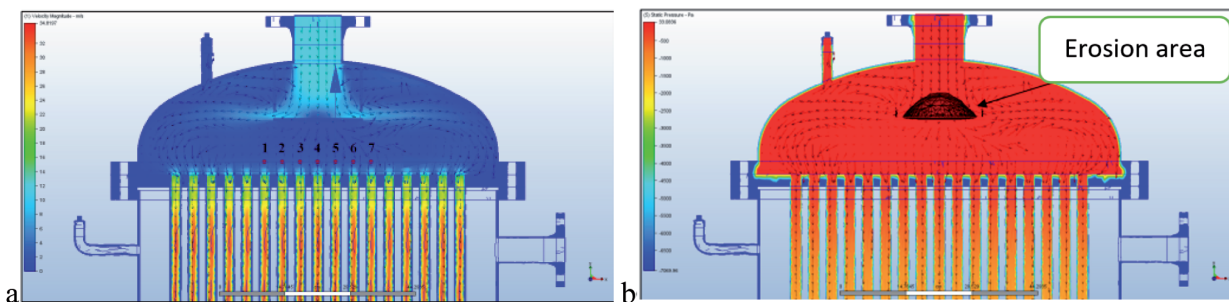
Fig. 10. **Distribution of water flow velocity (a) and pressure (b) in top head area of the condenser with dispersion plate**
Rys. 10.　Rozkład prędkości przepływu wody (a) i ciśnienia (b) w dennicy górnej kondensatora z płytą rozpraszającą
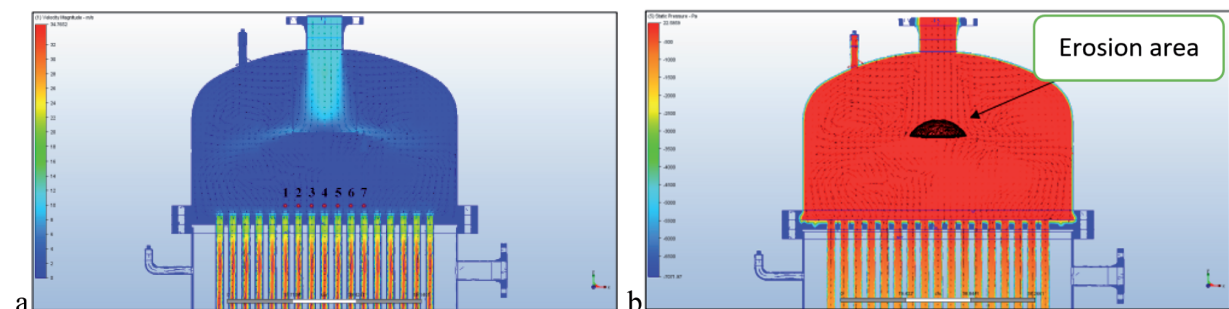

Fig. 11. **Distribution of water flow velocity (a) and pressure (b) in top head area of the condenser with its height increased by 250 mm and with a dispersion plate**
Rys. 11.　Rozkład prędkości przepływu wody (a) i ciśnienia (b) w dennicy górnej kondensatora ze zwiększoną jej wysokością o 250 mm i z płytą rozpraszającą
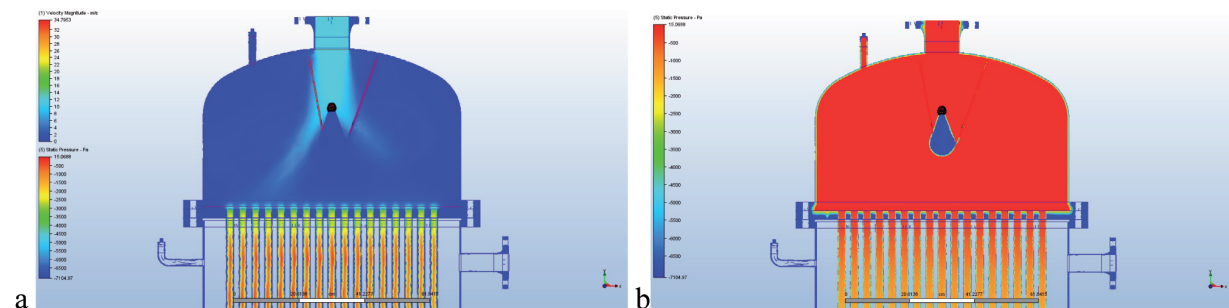

Fig. 12. **Distribution of water flow velocity (a) and pressure (b) in top head area of the condenser with the height increased by 250 mm and with a falling droplet shaped dispersion element**
Rys. 12.　Rozkład prędkości przepływu wody (a) i ciśnienia (b) w dennicy górnej kondensatora ze zwiększoną jej wysokością o 250 mm i z elementem rozpraszającym w kształcie spadającej kropli wody
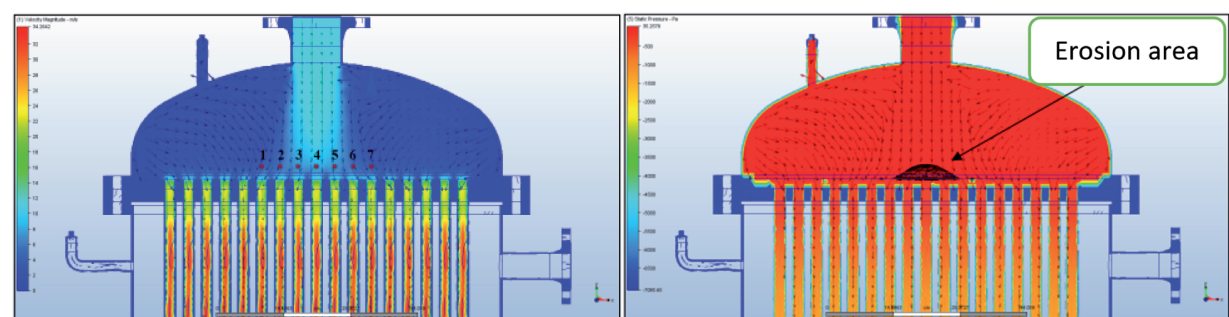

Fig. 13. **Distribution of water flow velocity (a) and pressure (b) in top head area of the condenser with its height unchanged but with an additional PA66 polyamide sieve plate**
Rys. 13.　Rozkład prędkości przepływu wody (a) i ciśnienia (b) w dennicy górnej kondensatora z niezmienioną jej wysokością, lecz z dodatkową płytą sitową z poliamidu PA66
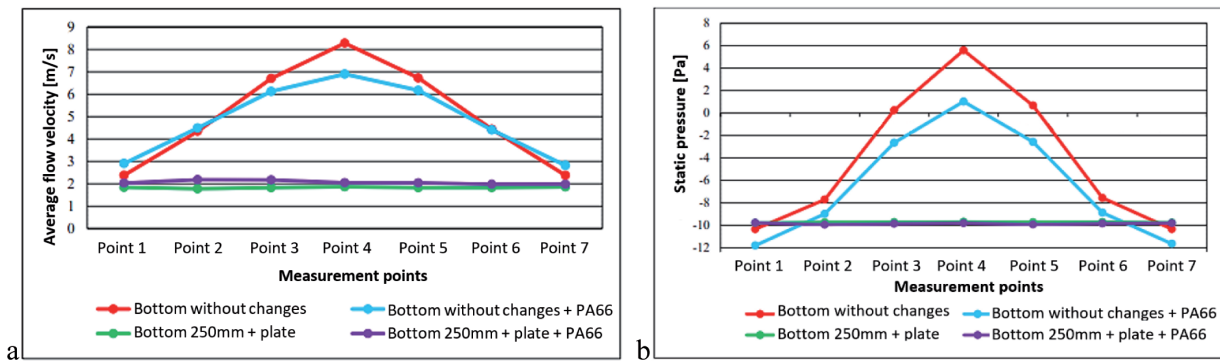
Fig. 14.   **Distribution of water flow velocity (a) and pressure (b) in selected points of the upper sieve plate of the condenser**
Rys. 14.   Rozkład prędkości przepływu wody (a) i ciśnienia (b) w wybranych punktach górnej płyty sitowej kondensatora

The effect in last tested variant of stream flow simulation in top head of the condenser with no change in height, but with an additional cover plate lying on top of the sieve plate is shown in **Fig. 13**. The plate has holes with the diameter corresponding to the inner diameter of the tubes, placed coaxially with them. The material of the tested plate was polyamide PA66 **[L. 20]**. Only the screen plate is subject to cavitational erosion and this element can be easily replaced when worn out. Damage to the upper sieve plate, caused by cavitational erosion, requires the replacement of the entire assembly consisting of top and bottom heads of the condenser together with the tubes.

Points 1–7 indicated in **Figs. 7–14** include the cavitation area in the operated sieve plate. **Figure 14** shows the distribution of water flow velocity (a) and pressure (b) at selected points on the upper sieve plate of the condenser. The data on the graph are for four variants: 1 – top head of the condenser unchanged, 2 – existing sieve plate with polyamide PA 66 protective plate, 3 – top head of the condenser elevated by 250 mm with dispersion plate, 4 – top head of the condenser elevated by 250 mm with dispersion plate and additional polyamide PA 66 protective plate. The compiled data shows that, under the given flow conditions, the upper sieve plate can be effectively protected against cavitational erosion when the top head of the condenser is elevated and a suspended dispersion plate is used (variant 3). Adding a protective sieve plate (variant 4) does not change the flow conditions, but provides additional protection against cavitation.

CONCLUSIONS

1. In the process of saturating wood with Creosote EN 13991WEI-C creosote oil, cavitational erosion of the upper sieve plate of the condenser was observed. The erosion affected the central part of the plate located below the inlet to the top head of the condenser. The erosion defects are concentrated at the weld connecting the tubes to the upper plate and inside the tube at a length of up to 60 mm.

2. During the saturation process under overpressure conditions, water squeezed out of the wood flows into the oil. In the final saturation stage, the resulting oil-water mixture is pushed into the heater. The residual mixture remaining in the cylinder and on the wood, in partial vacuum conditions, flows into the condenser. As water has a lower evaporation temperature, compared to creosote oil, it is the main cause of cavitational erosion of the upper sieve plate.

3. The analysis of the water flow in the DN800 condenser was carried out by a computer simulation using Autodesk Inventor Professional 2018 and additional CFD 2019 Ultimate software for numerical calculations and was performed with flow boundary conditions close to the real conditions. The analysis showed that the distribution of pressure and velocity of the water flow in the top head of the condenser was not uniform. Under these water flow conditions, the cavitation area occurred at the same location where erosion was found during condenser operation. This finding was the basis for the analysis of cavitation formation conditions in

the upgraded top head of the condenser during water flow under vacuum conditions.

4. The upgrade of the DN800 top head of the condenser consisted of: a – increasing the height of the top head of the condenser, b – installing a stream dispersion element between the stream inlet to the condenser and the top sieve plate, c – installing additional protective plate on the top sieve plate, in which the holes are concentric with the condenser tubes. Effects of the upgrade:

   a) after increasing the height of the top head of the condenser by 250 mm, a uniform stream velocity distribution over the upper sieve plate was not achieved, but no cavitation was observed at the inlet to the condenser tubes,

   b) the dispersion element in the form of a horizontal plate is exposed to intensive cavitational erosion, but protects the upper sieve plate from erosion; the dispersion element in the shape of a falling droplet causes uniform stream velocity over the upper sieve plate, no cavitation is observed at the sieve plate, however cavitational erosion of the top of the dispersion element is possible,

   c) additional protective plate is subject to cavitational erosion, but effectively protects the upper sieve plate from this process; the protective plate is a replaceable element.

5. A solution to increase the height of the top head of the condense and install an additional plate to protect the sieve plate is recommended for implementation studies.

REFERENCES

1. Brennen C.E.: Cavitation and Bubble Dynamics, Oxford University Press, 1995.
2. Bregliozzi G., Schino Di A., Ahmed S.I.U., Kenny J.M., Haefke H.: Cavitation wear behaviour of austenitic stainless steels with different grain sizes, Wear, Volume 258, 2005.
3. Li Z., Han J., Lu J., Zhou J., Chen J.: Vibratory cavitation erosion behavior of AISI 304 stainless steel in water at elevated temperatures, Wear, Volume 321, 2014.
4. Gągol M., Boczkaj G.: Przegląd metod wytwarzania kawitacji do degradacji zanieczyszczeń organicznych w środowisku wodnym, Aparatura Badawcza i Dydaktyczna 22, Gdańsk 2017.
5. Chao W., Duan A., Xu J., Liu X., Jin H., Ou G.: Cavitation failure analysis of 90-degree elbow of mixing point in ethylene glycol recovery and concentration system, Engineering Failure Analysis, Volume 125, 2021.
6. Dular M., Požar T., Zevnik J., Petkovšek R.: High speed observation of damage created by a collapse of a single cavitation bubble, Energy, Volume 418–419, 2019.
7. Li W., Lv Y., Sun Z., Yu W.: Cause analysis of corrosion leakage in convection section of ethylene cracking furnace, Engineering Failure Analysis, Volume 111, 2020. 109
8. Mychajło P., Kindrachuk M.: Trybologia, Politechnika Lubelska, Lublin 2017.
9. Xu W.L., Li J.B, Luo J., Zhai Y.W.: Effect of a single air bubble on the collapse direction and collapse noise of a cavitation bubble, Experimental Thermal and Fluid Science, Volume 120, 2021.
10. Li Z., Han J., Lu J., Zhou J., Chen J.: Vibratory cavitation erosion behavior of AISI 304 stainless steel in water at elevated temperatures, Wear, Volume 321, 2014.
11. Wojciechowski A., Doliński A., Radziszewska-Wolińska J.M., Wołosiak M.: Przyjazny dla środowiska recykling podkładów kolejowych, Problemy Kolejnictwa – Zeszyt 161, 2018.
12. Jaworska A., Milczarek D., Naduk E.: Impregnowanie drewnianych podkładów kolejowych z uwzględnieniem właściwości fizykochemicznych stosowanych środków ochrony drewna, Problemy kolejnictwa – Zeszyt 161, 2013.
13. Kowalik P., Fabijański M., Naduk E.: Requirements for wood products used in railway transport, WUT Journal of Transportation Engineering, Tom 129, 2020, p. 41.
14. Zastocki P.: Modernizacja konstrukcji rurowego wymiennika ciepła pracującego w warunkach zużycia kawitacyjnego. Praca dyplomowa. 2022. Białystok.
15. Jamroz S.: Krytyczne zjawiska związane z przepływem i sposoby ich ograniczania, Armatura i Rurociągi, październik – grudzień 2015, p. 11.

16. Zhang X.B., Qiu L.M., Qi H., Zhang X.J., Gan Z.H.: Modeling liquid hydrogen cavitating flow with the full cavitation model, International Journal of Hydrogen Energy, Volume 33, Wydanie 23, 2008.
17. Peters A., Sagar H., Lantermann U.: Ould el Mocta, Numerical modelling and prediction of cavitation erosion, Wear 338–339 (2015), pp. 189–201.
18. Petkovšek M., Dular M.: Simultaneous observation of cavitation structures and cavitation erosion, Wear, 2013, Volumen 300, pp. 55–64.
19. Chahine G.: Modeling of cavitation dynamics and interaction with material, in: Advanced Experimental and Numerical Techniques for Cavitation Erosion Prediction, Springer, Heidelberg, Germany, 2014 (ISBN 978-94-017- 8538-9).
20. Hattori S., Itoh T.: Cavitation erosion resistance of plastics, Wear, Volume 271, 2011.